Crustal deformation studies in Krafla, Gjástykki, Bjarnarflag and Þeistareykir areas utilizing GPS and InSAR

Status report for 2012

Vincent Drouin, Sigrún Hreinsdóttir
Karsten Spaans and Freysteinn Sigmundsson

Nordic Volcanological Center
Institute of Earth Sciences Report 1301
University of Iceland

Contents

Chapter 1

Introduction

Crustal deformation studies at Krafla, Þeistareykir, Gjástykki, and Bjarnarflag geothermal areas in the Northern Volcanic Zone (NVZ) were continued in 2012, utilizing Global Positioning System (GPS) geodesy and Interferometric Synthetic Aperture Radar (InSAR) analyses. Results from earlier studies include:

- Krafla: The most recent volcanic activity in the area was the Krafla rifting episode 1975-1984. Gradual uplift continued until 1989, five years after the last eruption, due to pressure increase in the shallow magma chamber under the center of the Krafla caldera. In 1989, the area begin to subside at a fast rate of more than 5 cm/yr. The rate of subsidence decayed at an exponential rate. The estimated subsidence rate in 2006 was lower than 3 mm/yr [Sturkell et al., 2008].

  Following this development, the area of maximum rate of subsidence shifted 1.6 km SSE, from being directly above the shallow magma chamber, towards the array of boreholes in the Leirbotnar area. Similar subsidence has been observed around the array of boreholes at Bjarnarflag [Sturkell et al., 2008].

  A broad uplift signal has also been detected north and north-east of Krafla. Initially this was only detected during the 1990s, but recent processing results have shown that the signal persisted in the 2003-2010 period [Spaans et al., 2012]. Candidate explanations include magma accumulation near the crust/mantle boundary and/or post-rifting relaxation.

  Plate spreading across the NVZ and associated subsidence along the Krafla fissure swarm produce a clear deformation signal.

- Þeistareykir: Inflation of the area is observed from 2007-2008 suggesting magma intrusion [Metzger et al., 2011; Spaans et al., 2012].

- Glacial isostatic adjustment needs to be considered as well, because ongoing retreat of ice caps in Iceland is influencing the area [Árnadóttir et al., 2009; Auriac et al., 2013].

The present report describes results from applying GPS and InSAR techniques in the Krafla and Þeistareykir areas. It describes both GPS campaign measurements carried out in 2012 as well as continuous measurements, including the installation of one new continuous GPS station in Bjarnarflag (Chapter 2). An overview is also presented on satellite synthetic aperture radar (SAR) data (Chapter 3) acquired 2009-2012 for the purpose of carrying out interferometric analysis (InSAR).

Chapter 2

GPS

GPS campaign measurements were carried out in July, August, and late November 2012. A total of 79 stations were measured in Krafla, Gjástykki, Bjarnarflag, and Þeistareykir areas. Furthermore, a new continuous GPS station, named BJAC, was installed in Bjarnarflag, east of lake Myvatn.

GPS instruments used for the measurements are from the Institute of Earth Sciences (IES), UNAVCO, and King Abdullah University of Science and Technology (KAUST).

- Receivers: Trimble 5700, R7 and NET R9.
- Antennas: Trimble Zephyr Geodetic (TRM41249.00) and Trimble Zephyr Geodetic II (TRM57971.00).

Each campaign GPS station was measured for at least 24 hours, sampling data every 15 seconds.

The following people participated in the 2012 GPS measurements: From IES: Karsten Spaans, Sveinbjörn Steinþórsson, Vincent Drouin, Halldór Ólafsson, Karolina Michalczewska, Ásta Rut Hjartardóttir, Amandine Auriac, Freysteinn Sigmundsson, Sigrún Hreinsdóttir. From Gothenburg University, Sweden: Erik Sturkell

The data were analyzed at the University of Iceland using the GAMIT/GLOBK analysis software [Herring et al., 2010a; Herring et al., 2010b] using over 100 global reference stations to determine stations coordinates in the ITRF08 reference frame.

The resulting coordinates of the 79 GPS stations measured are presented in Table 2.2.

2.1 Summer 2012 GPS campaign

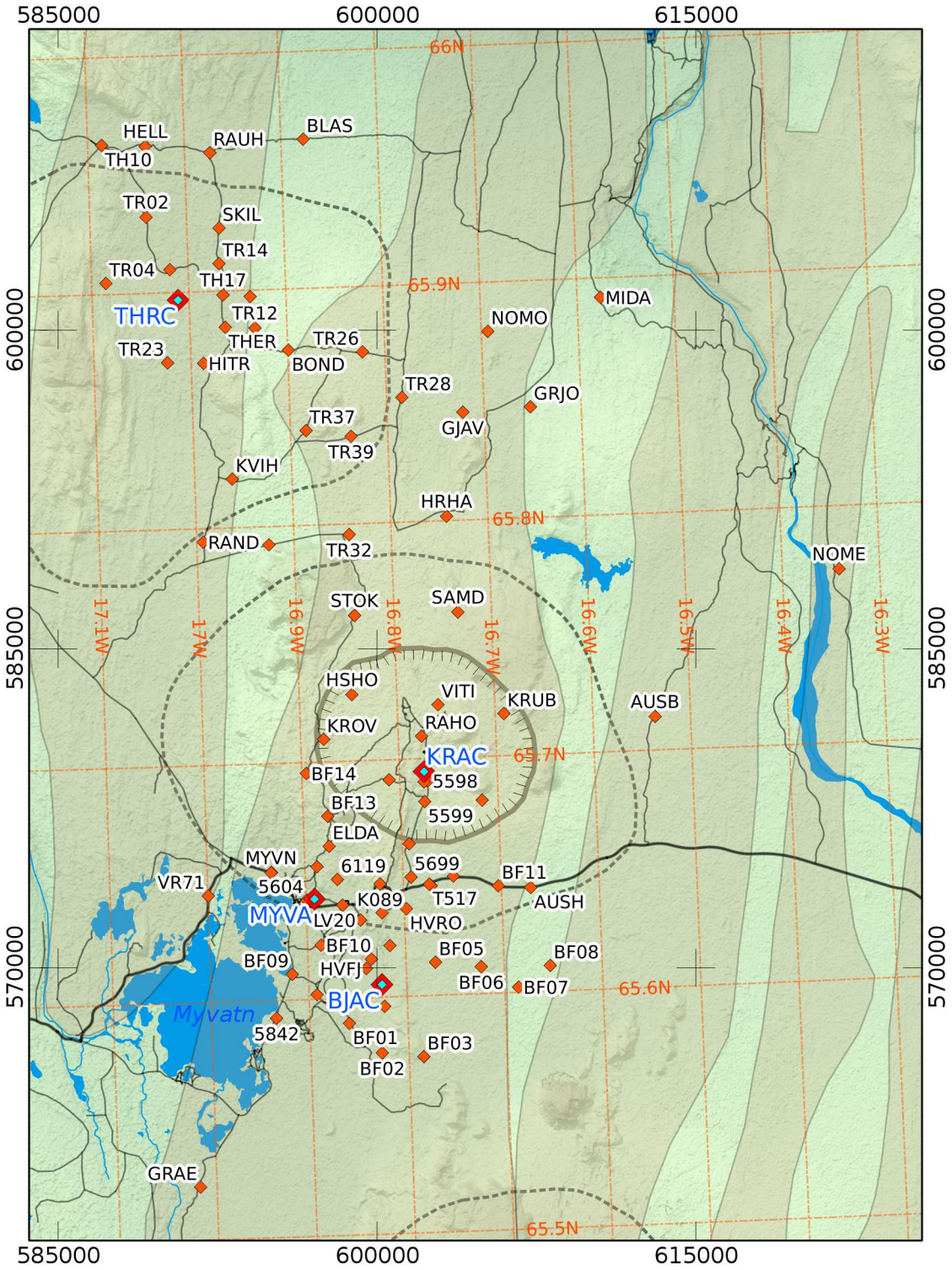

Figure 2.1: Map of measured GPS stations. Red diamonds show campaign GPS sites ; red diamonds with blue core show continuous GPS sites. Map reference system: ISN93. Background map shows volcanic systems [Einarsson and Sæmundsson, 1987; Hjartardóttir et al., 2012]: fissure swarms (light brown), approximate extent of the Þeistareykir, Krafla, and Fremri-Námar central volcanoes (dashed lines) and the Krafla caldera (comb line).

ID	Latitude	Longitude	Height	X	Y	Z	Date
0205	65.60195748	-16.89195612	350.134	2528131.143	-767717.293	5786073.318	2012.618
5598	65.69055026	-16.77138313	509.655	2521187.033	-759817.438	5790292.421	2012.822
5599	65.68187686	-16.77528283	460.585	2521959.857	-760237.591	5789849.481	2012.623
5603	65.63937937	-16.86281822	384.852	2524897.612	-765333.133	5787827.392	2012.619
5604	65.64198129	-16.89909985	361.126	2524150.213	-766852.155	5787925.447	2012.619
5697	65.66427896	-16.79262862	446.943	2523436.069	-761516.035	5789028.674	2012.817
5699	65.65018979	-16.79194209	427.233	2524807.789	-761896.981	5788363.125	2011.974
5842	65.59259249	-16.93399197	360.702	2528481.138	-769850.148	5785651.504	2012.822
6119	65.65026798	-16.86723962	407.490	2523788.940	-765209.732	5788348.734	2012.822
6122	65.61621454	-16.83531483	432.316	2527535.500	-764808.154	5786804.682	2012.623
6123	65.65001381	-16.74868864	425.080	2525398.506	-759995.645	5788353.072	2012.622
7157	65.69157574	-16.81095804	537.220	2520572.718	-761531.813	5790364.616	2012.819
AUSB	65.71411601	-16.53631637	478.451	2521974.773	-748782.076	5791345.284	2011.972
AUSH	65.64397832	-16.67009560	432.050	2527028.739	-756707.532	5788081.899	2012.821
BF01	65.58941158	-16.85993998	353.757	2529780.382	-766674.414	5785498.603	2012.617
BF02	65.57649004	-16.82753558	420.175	2531495.668	-765631.298	5784963.466	2012.618
BF03	65.57430145	-16.78524775	426.017	2532275.113	-763827.556	5784867.873	2012.618
BF04	65.59608529	-16.82340180	437.239	2529653.140	-764874.840	5785882.132	2012.618
BF05	65.61394199	-16.77004924	417.313	2528620.109	-761993.351	5786686.393	2012.618
BF06	65.61134946	-16.72353572	433.935	2529496.607	-760018.070	5786582.165	2012.622
BF07	65.60221649	-16.68620300	435.062	2530880.171	-758636.189	5786162.591	2012.622
BF08	65.61083001	-16.65316899	437.286	2530479.968	-756926.459	5786561.299	2012.622
BF09	65.61088039	-16.91656336	349.547	2526934.019	-768539.256	5786483.709	2012.625
BF10	65.62280594	-16.88610722	352.648	2526184.449	-766844.490	5787035.521	2012.816
BF11	65.64520205	-16.70310574	431.669	2526473.135	-758127.543	5788137.826	2012.819
BF12	65.65592837	-16.88766669	439.451	2522978.319	-765946.241	5788638.066	2012.819
BF13	65.67703052	-16.87504711	520.788	2521127.280	-764777.863	5789681.774	2012.819
BF14	65.69541500	-16.89538158	624.173	2519108.800	-765141.977	5790620.086	2012.819
BF18	65.62166600	-16.81597474	434.156	2527264.241	-763794.986	5787057.296	2012.583
BLAS	65.96293089	-16.87684574	332.983	2493198.100	-756391.083	5802569.209	2011.909
BOND	65.87420078	-16.89934058	564.981	2501634.912	-760023.350	5798743.653	2011.460
BOTF	65.68159317	-16.71654480	568.255	2522807.980	-757672.795	5789934.571	2012.576
ELDA	65.66438172	-16.87455771	462.379	2522340.669	-765122.414	5789047.462	2012.568
GJAV	65.84548770	-16.72192616	474.543	2506739.227	-753103.562	5797351.633	2011.963
GRAE	65.52241731	-17.01680751	351.571	2534173.986	-775587.689	5782405.352	2012.025
GRJO	65.84670858	-16.65220890	458.036	2507528.258	-750015.282	5797392.280	2011.904
HELL	65.96203198	-17.04040697	339.614	2491118.798	-763532.898	5802534.434	2012.009
HITR	65.86977465	-16.98710005	392.432	2500831.201	-763965.187	5798384.416	2012.031
HRHA	65.80182507	-16.74253189	563.713	2510756.821	-755295.144	5795438.904	2011.553
HSHO	65.72801300	-16.84595016	611.461	2516591.785	-762006.623	5792103.732	2012.081
HVFJ	65.61227228	-16.84074053	422.386	2527842.349	-765162.306	5786614.137	2012.583
HVIT	65.69021830	-16.77528347	517.184	2521170.572	-759999.694	5790284.043	2011.619
HVRO	65.63695243	-16.79783691	428.664	2526017.292	-762545.528	5787755.670	2012.577
K089	65.64778152	-16.82382576	490.725	2524642.664	-763380.244	5788310.240	2012.622
KROV	65.70955595	-16.87657659	642.408	2517991.634	-763900.075	5791285.567	2012.568
KRUB	65.71779175	-16.69100823	693.578	2519670.822	-755506.475	5791709.950	2012.577
KVIH	65.82057611	-16.96151171	466.029	2505989.093	-764317.391	5796206.572	2012.132
LV20	65.63282450	-16.84492425	398.808	2525779.283	-764739.163	5787538.575	2012.130
MIDA	65.89174624	-16.57579582	379.915	2504102.750	-745353.746	5799374.197	2011.915
MY24	65.65416806	-16.93434527	358.224	2522492.519	-768043.782	5788483.144	2012.816
MYVN	65.65404656	-16.93479904	358.381	2522498.307	-768067.374	5788477.702	2012.059
NAMA	65.63560298	-16.82280164	550.220	2525864.010	-763700.268	5787804.325	2012.816
NEW2	65.64624750	-16.77159450	424.293	2525460.500	-761115.508	5788179.181	2012.587
NOME	65.77322683	-16.34166810	430.530	2518718.289	-738513.551	5794009.528	2011.977
NOMO	65.87919404	-16.69327808	467.794	2503827.305	-750864.014	5798882.527	2011.815
RAHO	65.70950595	-16.77623273	623.364	2519322.980	-759488.275	5791265.916	2012.051
RAND	65.79436215	-16.99340369	463.925	2508112.480	-766491.207	5795006.717	2011.909
RAUH	65.95851034	-16.97371802	347.993	2492352.106	-760738.561	5802382.109	2012.029
SAMD	65.76125178	-16.73439655	678.067	2514860.533	-756140.259	5793687.153	2012.576
SKHO	65.90972973	-17.01883747	356.771	2496505.007	-764155.778	5800171.904	2011.931
SKIL	65.92666317	-16.96676681	361.739	2495551.477	-761384.144	5800946.940	2011.865
STOK	65.76133784	-16.84052702	582.466	2513409.660	-760783.396	5793603.920	2012.079
T517	65.64695839	-16.77350996	425.040	2525366.203	-761179.184	5788212.550	2012.623
TH17	65.89833595	-16.96485433	389.793	2498346.134	-762145.630	5799683.327	2012.295
THER	65.88470321	-16.96363695	401.571	2499694.175	-762498.809	5799073.118	2012.040

Table 2.2: 2012 GPS coordinates given in the ITRF08 reference system. Latitude and longitude are in decimal degrees. Height and cartesian coordinates are in meters. Date is in decimal year. Notice that BOTF is also known as BF15, HVRO as BF16 and HVFJ as BF17.

2.2 Continuous GPS stations

Continuous GPS measurements allow us to better quantify and understand time dependent and secular deformation signals. In Iceland we have several sources of crustal deformation. Plate spreading, glacial isostasy, earthquakes, volcanic activity, and changes in geothermal fields (including changes due to utilization) are among different sources we can expect in the NVZ. In order to better understand and distinguish between the different sources and detect and understand transient signals we need to have both good spatial and time resolution of geodetic data. Campaign GPS and InSAR data provide us with good spatial resolution and the continuous GPS stations help resolve time dependent signals and improve accuracy of network solutions.

A new continuous GPS station, named BJAC, was installed in Bjarnarflag, on 25 October 2012 by Sveinbjörn Steinþórsson and Karsten Spaans from IES (Fig. 2.2). Time series of the data gathered since the installation are shown in Figure 2.3.

Figure 2.2: Picture of Bjarnarflag continuous GPS station (BJAC). It is supplied with both wind and solar energy.

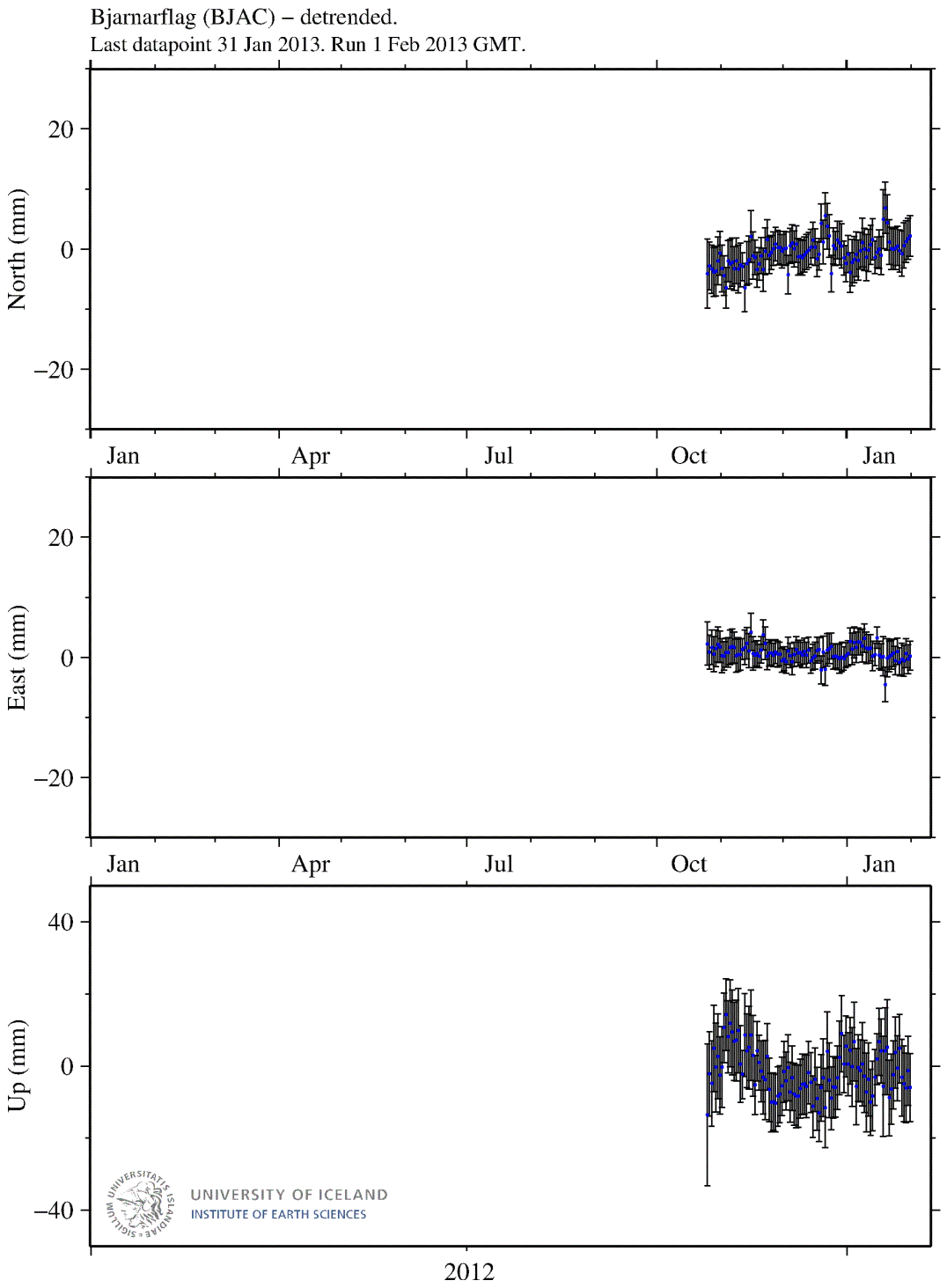

Figure 2.3: GPS time series for Bjarnarflag GPS station. Displacements are presented in the ITRF08 reference frame subtracting velocities of 22.5 mm/yr, 0.8 mm/yr and 0.5 mm/yr in the north, east and up components. The time series are too short to evaluate BJAC velocity in ITRF08 so we assumed the values to be the same as for the nearest continuous GPS station, MYVA.

In addition, there are three other continuous GPS stations:

- THRC: Installed in Þeistareykir on 1 September 2011 by the Institute of Earth Sciences.
- KRAC: Installed in Krafla on 8 November 2011 by the Institute of Earth Sciences.
- MYVA: Installed near Myvatn on 31 August 2006 by Christof Völksen form the Commission for Geodesy and Glaciology, Bavarian Academy of Sciences and Humanities.

The data were analyzed at the University of Iceland using the GAMIT/GLOBK 10.4 analysis software using over 100 global reference stations to determine stations coordinates in the ITRF08 reference frame. We show detrended time series for the North, East and Up components. The trend of each component (East, North and Up) is computed (by minimizing the standard deviation) and subtracted from the time series. The trends give us the average velocities in each direction. When the average velocity is subtracted from the time series, it is flattened.

Detrended GPS time series from these sites are shown in Figs 2.4, 2.5 and 2.6. None of them is showing any significant deviations from the zero value that would relate to unusual deformation or displacements rate deviating from linear trends. The data from the continuous sites provides excellent reference to check for future irregularities of displacements that may arise from e.g. future utilization of the area.

The following velocities have been calculated for each continuous GPS station:

	North [mm/year]	East [mm/year]	Upp [mm/year]
THRC	21.3 ± 0.3	-5.6 ± 0.3	3.1 ± 1.0
KRAC	23.1 ± 0.3	0.4 ± 0.3	-1.9 ± 1.4
MYVA	22.5 ± 0.1	0.8 ± 0.1	0.5 ± 0.3

Table 2.3: Station velocities in the ITRF08 reference system.

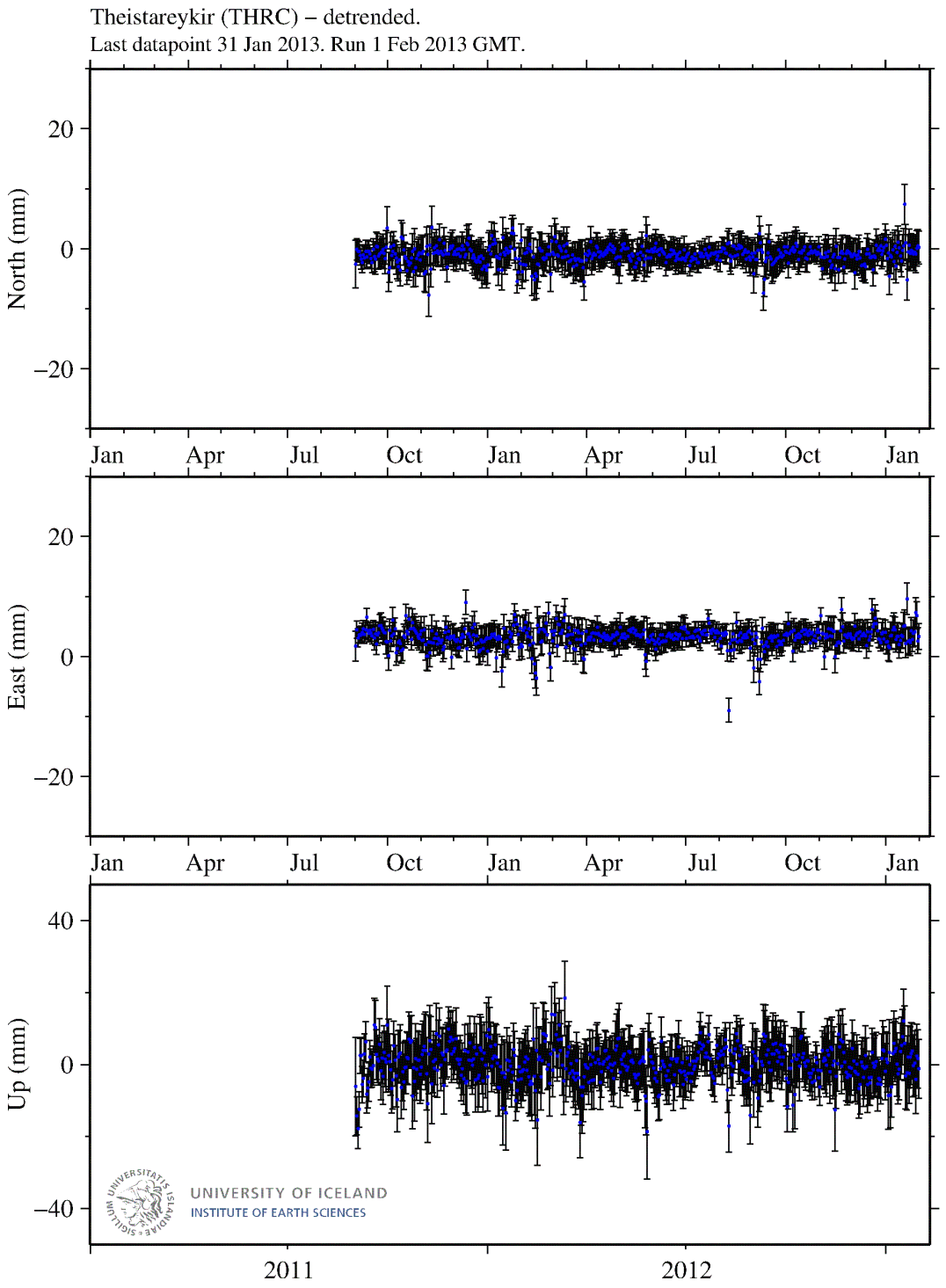

Figure 2.4: GPS time series for the Þeistareykir GPS station. Displacements are detrented using secular velocities of 21.3 mm/yr, -5.6 mm/yr and 3.1 mm/yr in the ITRF08 and annual and semi-annual terms estimated using time series analysis.

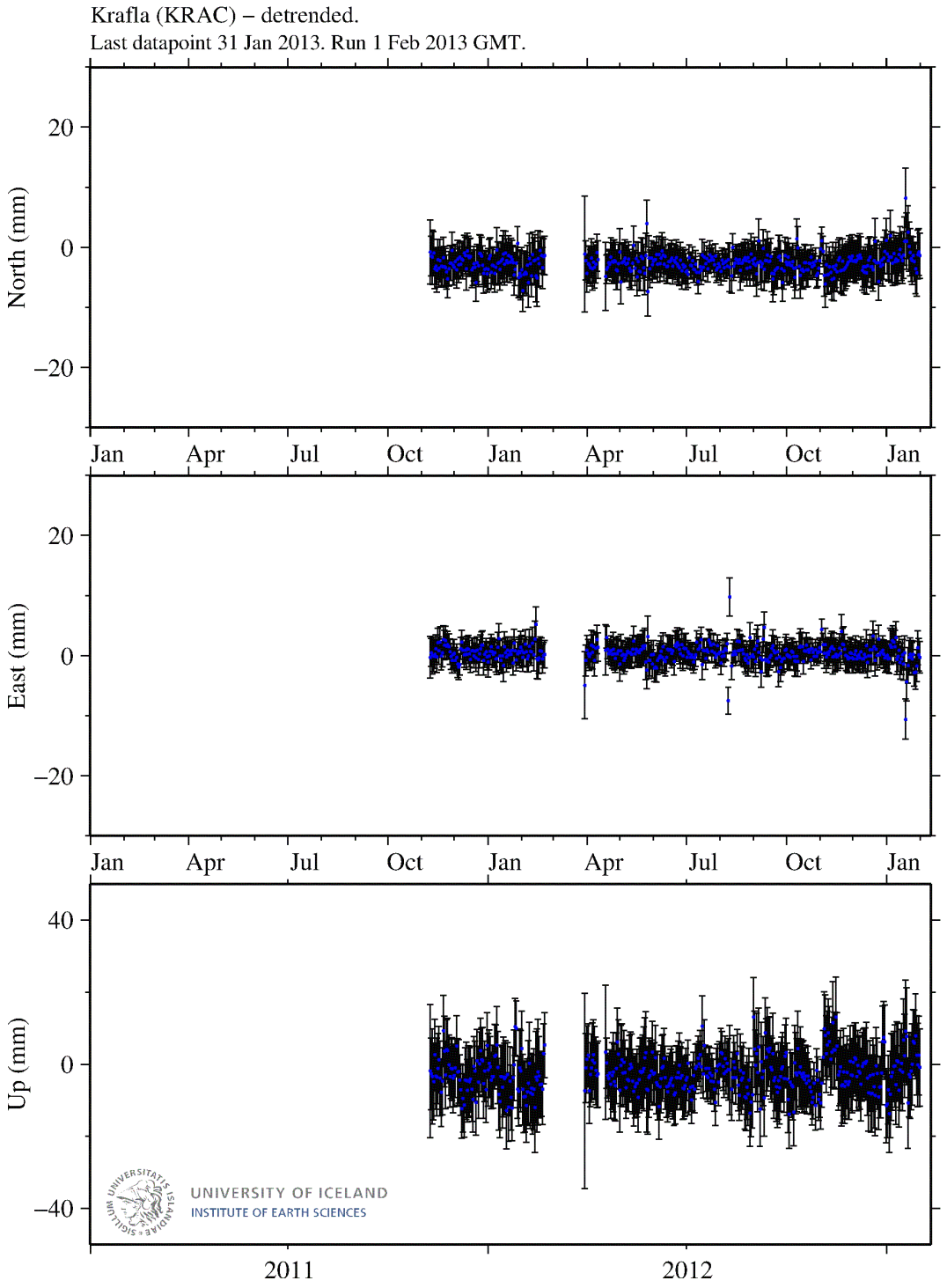

Figure 2.5: GPS time series for the Krafla GPS station. Displacements are detrented using secular velocities of 23.1 mm/yr, 0.4 mm/yr and -1.9 mm/yr in the ITRF08 and annual and semi-annual terms estimated using time series analysis.

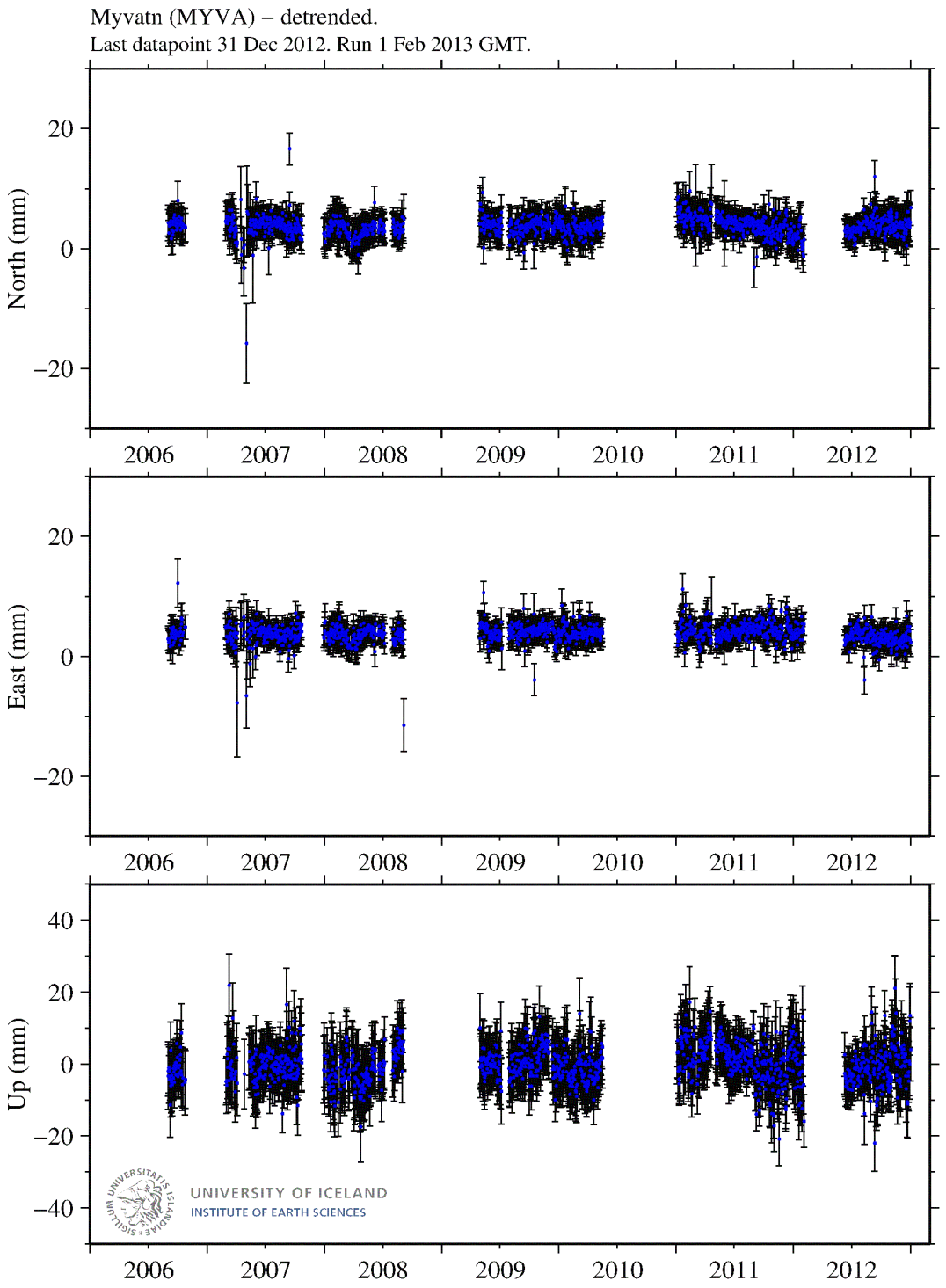

Figure 2.6: GPS time series for the Myvatn GPS station. Displacements are detrented using secular velocities of 22.5 mm/yr, 0.8 mm/yr and 0.5 mm/yr in the ITRF08 and annual and semi-annual terms estimated using time series analysis.

2.3 Velocity field 2010-2012

A velocity field has been calculated based on the GPS data collected in 2010, 2011 and 2012 (Figs 2.7 and 2.8). Velocities were initially estimated in the ITRF08 reference frame. Then, using the ITRF2008 plate motion model [Altamimi et al., 2012], they are converted into velocities relative to the Eurasian plate or the North-American plate.

Velocities relative to a particular plate allow, in our case, the determination of the style of stretching across the NVZ and, furthermore, to check if other other deformation sources in addition to plate stretching are active. At the NVZ divergent plate boundary, the full relative plate velocity is 18.6 mm/yr according the NUVEL-1A model [DeMets et al., 1990; DeMets et al., 1994], with an azimuth of 105/285 degrees, depending on which plate is the reference.

Vertical velocities are independent of any reference plate. Detailed map of the vertical velocities for Krafla and Þeistareykir areas are available (Figs 2.10 and 2.13).

Only the GPS velocities with an uncertainty of 1 cm or better in the vertical component are shown in all the following figures.

2.3.1 North-American plate as reference

GPS stations near Húsavík show little velocity relative to stable North-American plate (Fig 2.7). However, there appears to be some effect of the Húsavík-Flatey fault, which is a right-lateral transform fault. GPS station south of Húsavík are moving north-west while GPS stations north of the village are moving north-east.

The whole data set shows well how eastward horizontal velocities increase gradually across the plate boundary, from west to east across the swarms marking the plate boundary. For example, the horizontal velocities are only few mm/yr near Húsavík but reach full plate velocities at the NOME benchmark to the east of the plate boundary.

Detailed maps of the horizontal velocities relative to the North-American plate for Krafla and Þeistareykir areas are shown in Figs 2.9 and 2.12.

2.3.2 Eurasian plate as reference

By changing the reference plate to Eurasia, the velocity field is “reversed”. Horizontal velocities now gradually increase towards the west.

The NOME station, the most easterly GPS station, is not showing any velocity in the horizontal component (Fig 2.8). It is following exactly the same motion as the Eurasian plate. This means the GPS benchmark is located on a stable part of the plate. On the other plate, near Húsavík the velocities are about 14-15 mm/yr.

Detailed map of the horizontal velocities relative to the Eurasian plate for Krafla and Þeistareykir areas are shown in Figs 2.10 and 2.13.

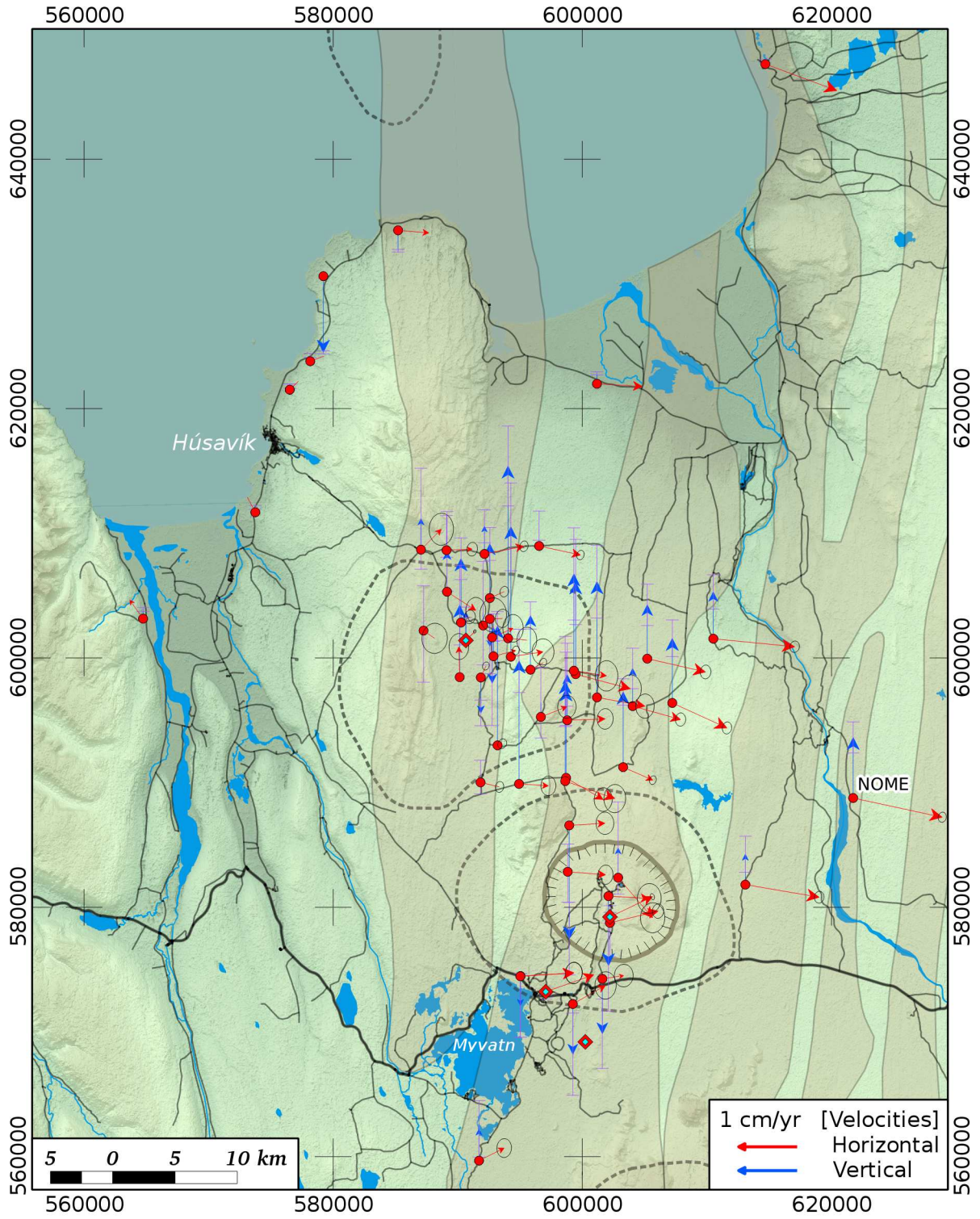

Figure 2.7: GPS velocities relative to stable North-American plate. Map reference system: ISN93. Background is same as Fig 2.1. Ellipses at arrow heads show 95% confidence intervals.

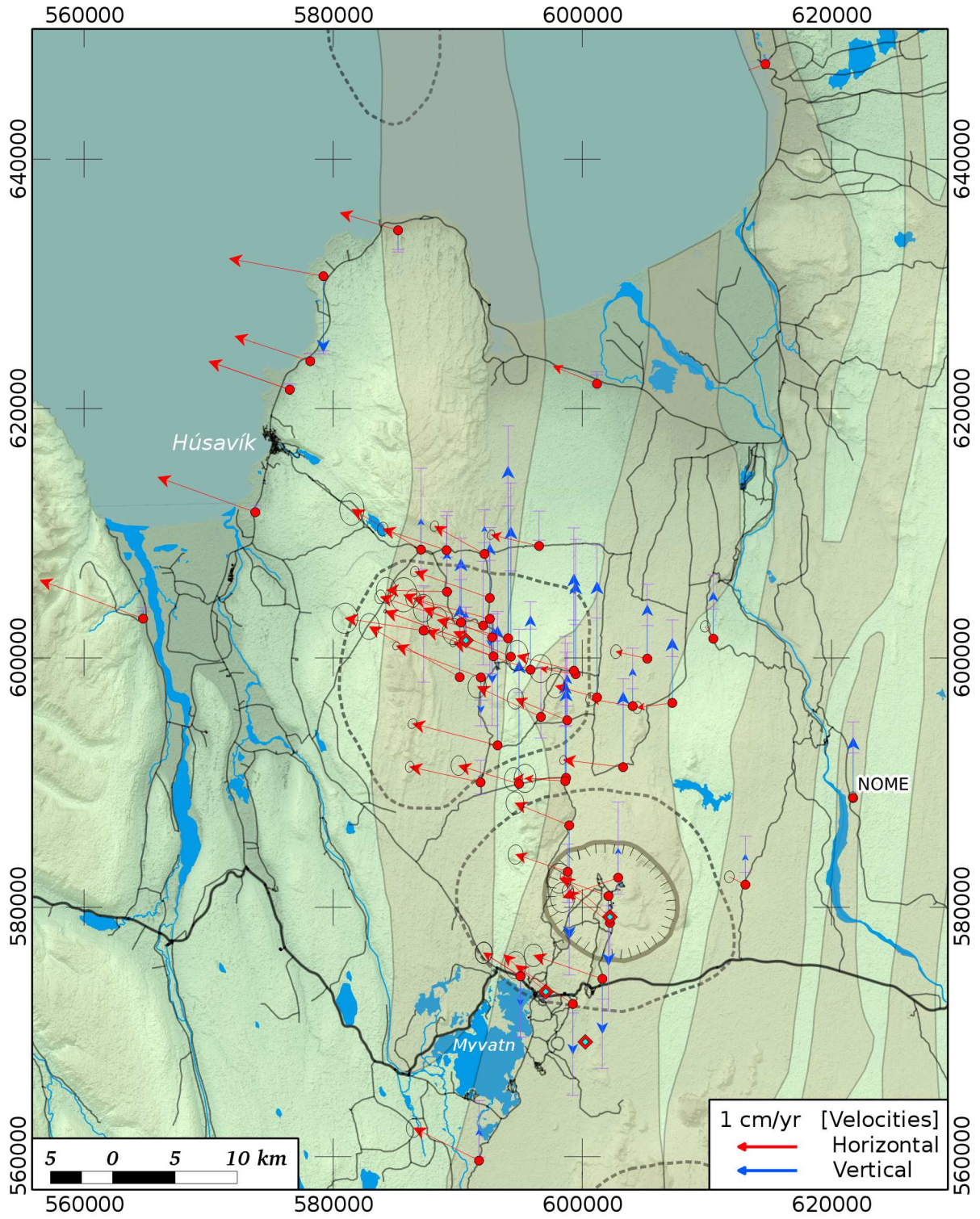

Figure 2.8: GPS velocities relative to stable Eurasian plate. Map reference system: ISN93. Background is same as Fig 2.1. Ellipses at arrow heads show 95% confidence intervals.

2.3.3 Velocities in the Krafla area

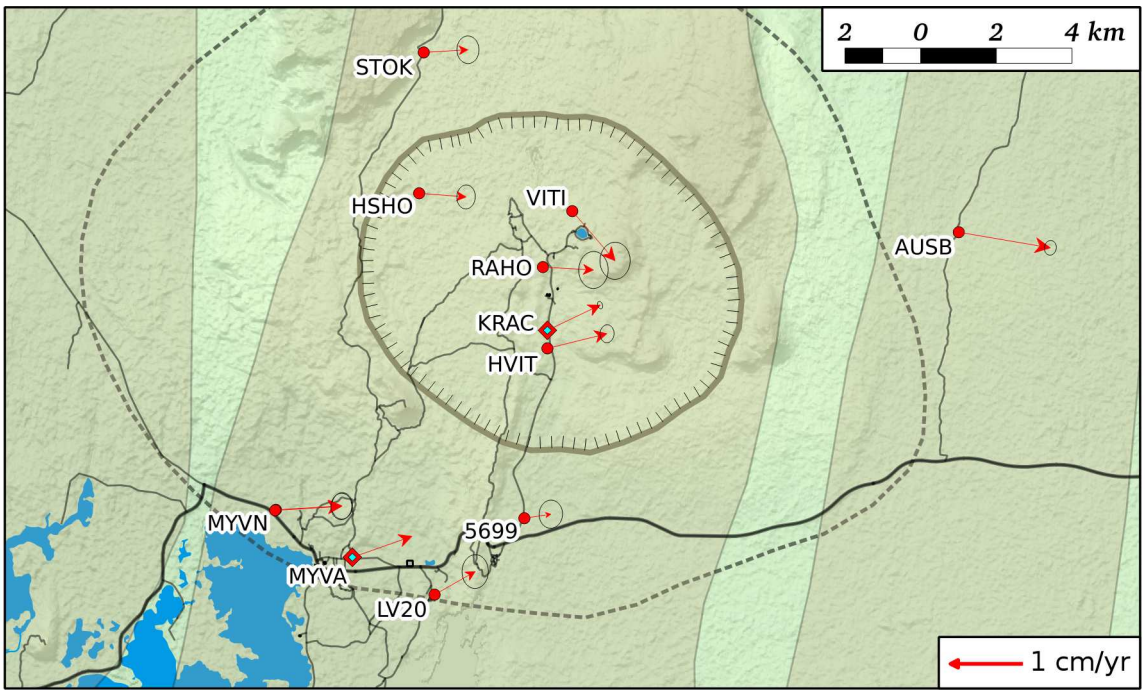

Figure 2.9: Horizontal GPS velocities in the Krafla area relative to stable North-American plate. Background is same as Fig 2.1. Ellipses at arrow heads show 95% confidence intervals.

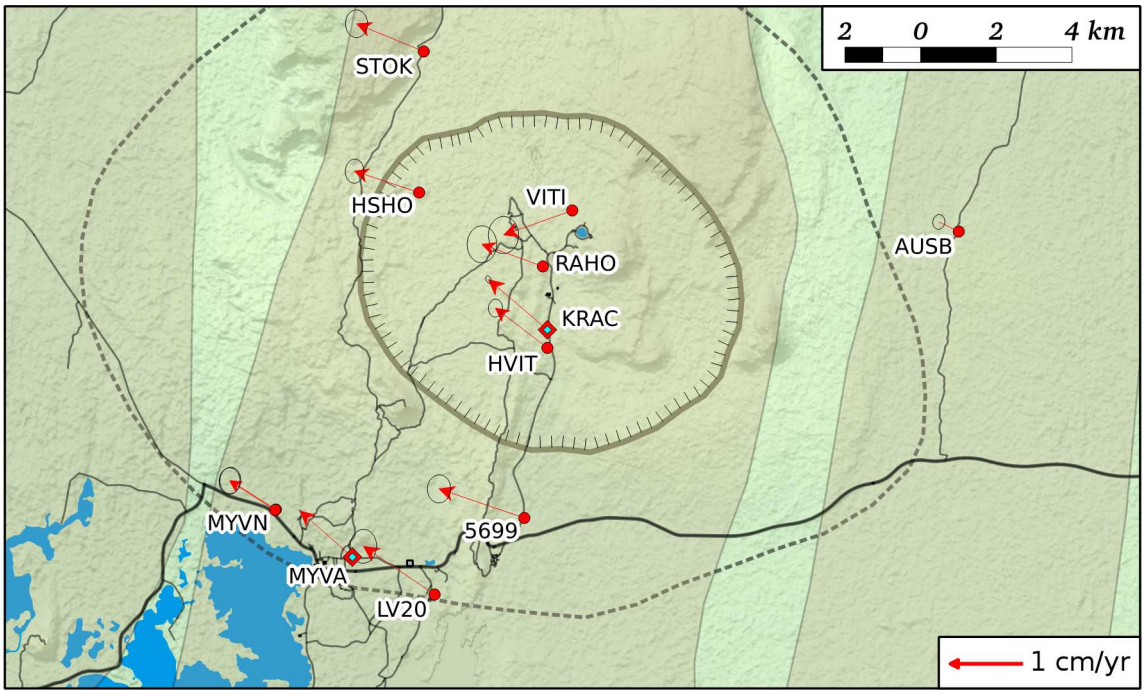

Figure 2.10: Horizontal GPS velocities in the Krafla area relative to stable Eurasian plate. Background is same as Fig 2.1. Ellipses at arrow heads show 95% confidence intervals.

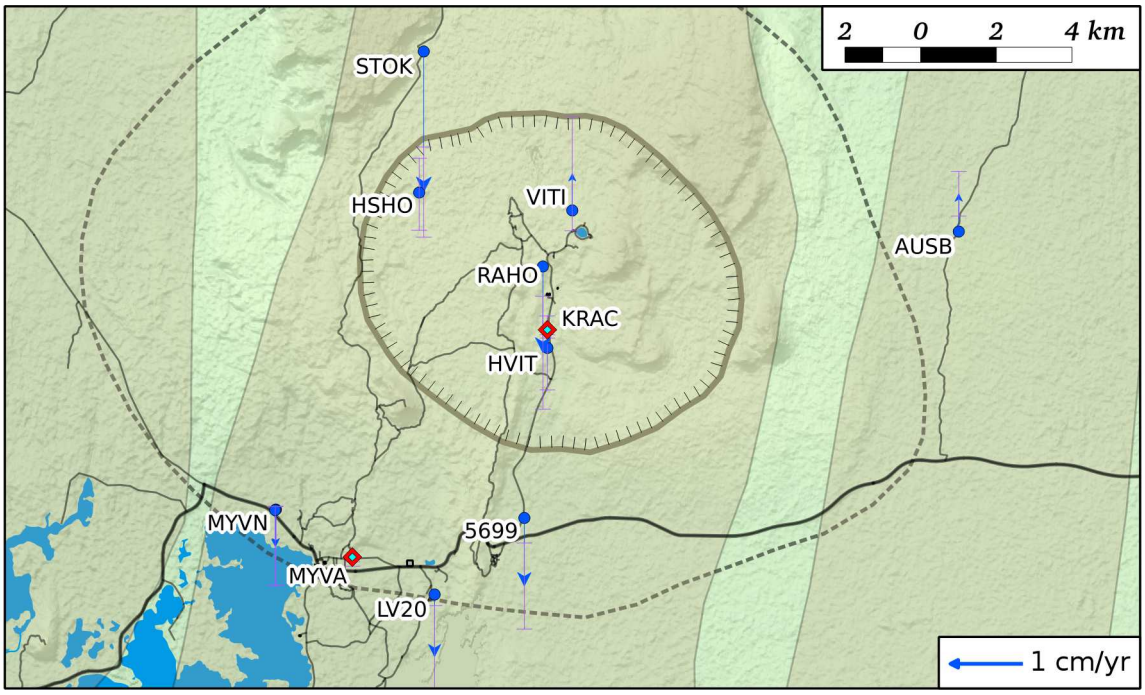

Figure 2.11: Vertical GPS velocities in the Krafla area. Background is same as Fig 2.1. Ellipses at arrow heads show 95% confidence intervals.

2.3.4 Velocities in the Þeistareykir area

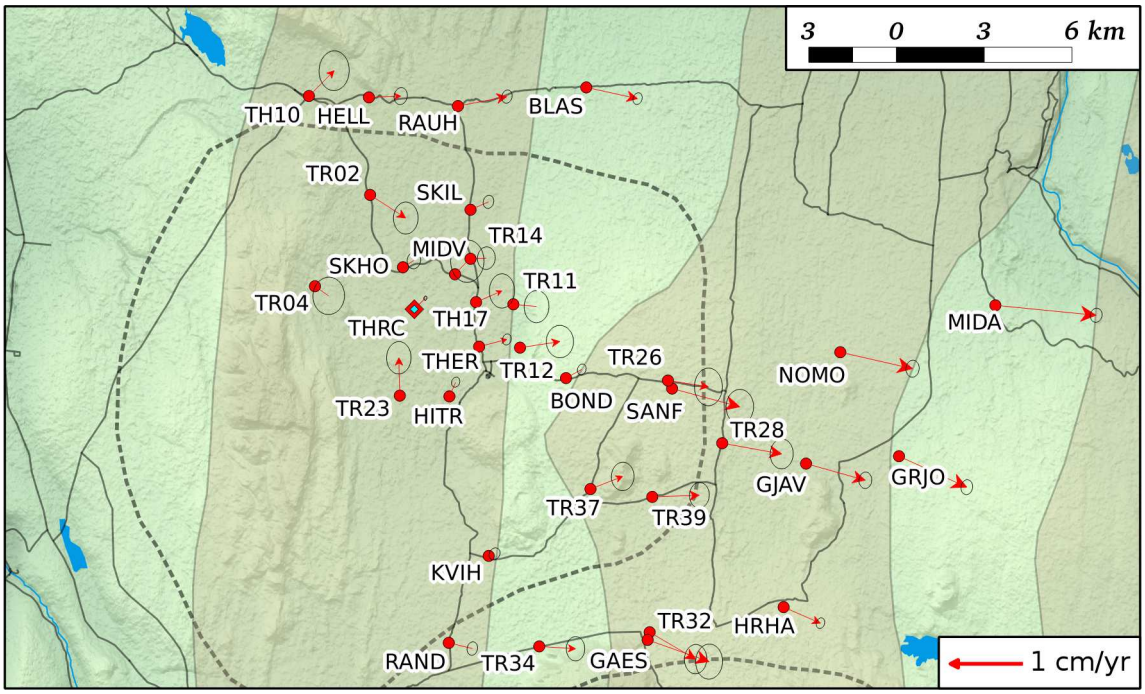

Figure 2.12: Horizontal GPS velocities in the Þeistareykir area relative to stable North-American plate. Background is same as Fig 2.1. Ellipses at arrow heads show 95% confidence intervals.

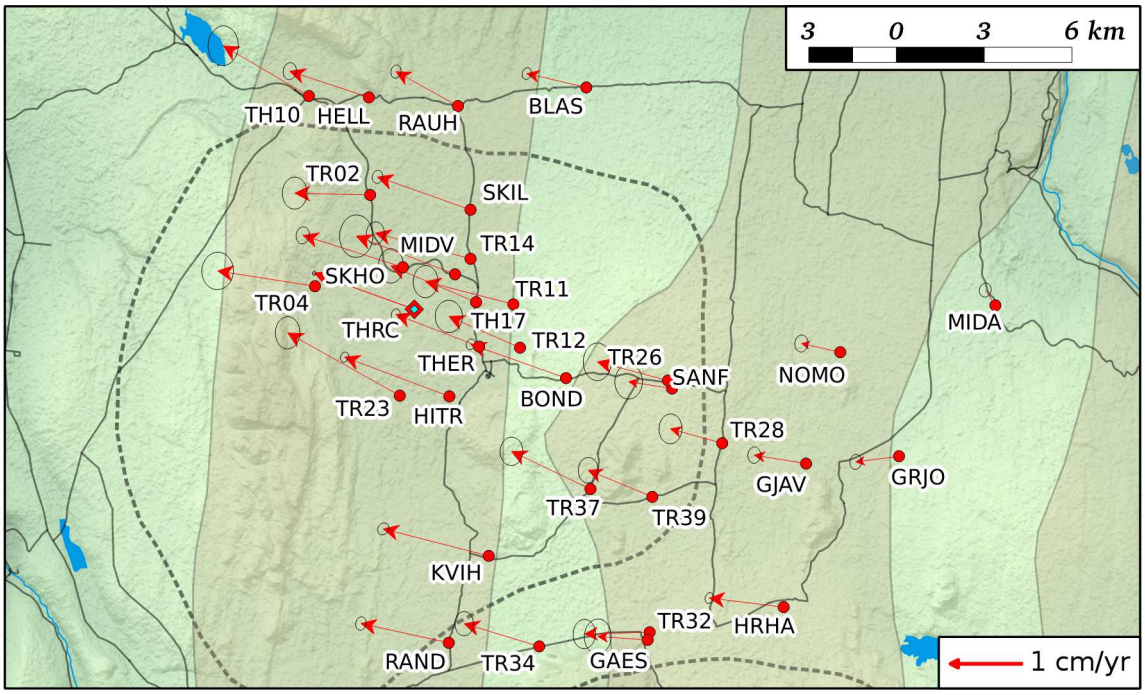

Figure 2.13: Horizontal GPS velocities in the Þeistareykir area relative to stable Eurasian plate. Background is same as Fig 2.1. Ellipses at arrow heads show 95% confidence intervals.

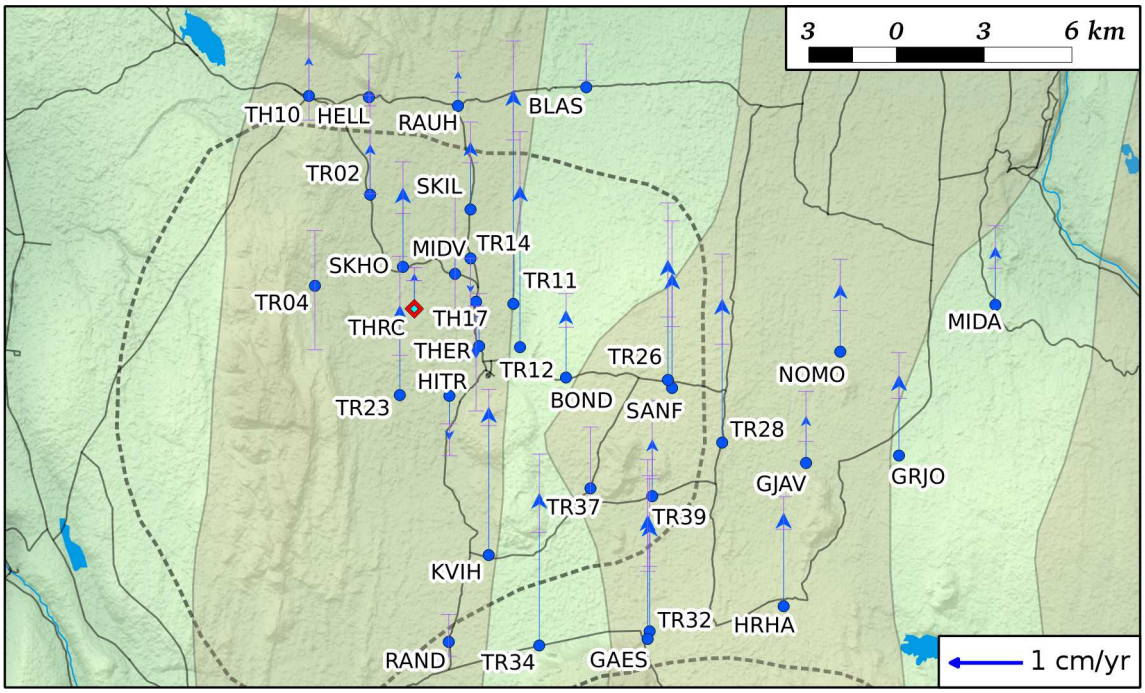

Figure 2.14: Vertical GPS velocities in the Þeistareykir area. Background is same as Fig 2.1. Ellipses at arrow heads show 95% confidence intervals.

2.3.5 Interpolation of the 2010-2012 velocity field

Velocities have been interpolated using regularized spline with tension (RST). This is an interpolation method which aims to pass trough (or close to) the input data points and at the same time make the resulting surface as smooth as possible [Cebecauer et al., 2002]. RST has been chosen instead of other methods because of our GPS velocities network: GPS benchmarks do not coincide with maximum displacements. The velocity field is also assumed to be a smooth surface with no ruptures in it as there was no known faulting events during the 2010-2012 time period.

The interpolation has been done with velocities relative to stable Eurasian plate. Zero velocity means then that the station is moving in the same manner as the stable interior of the Eurasian plate. The ITRF08-EURA velocity of a GPS station on the other side of the plate boundary, within the stable interior of the North American Plate would be 18.6 mm/yr in direction 285 degrees.

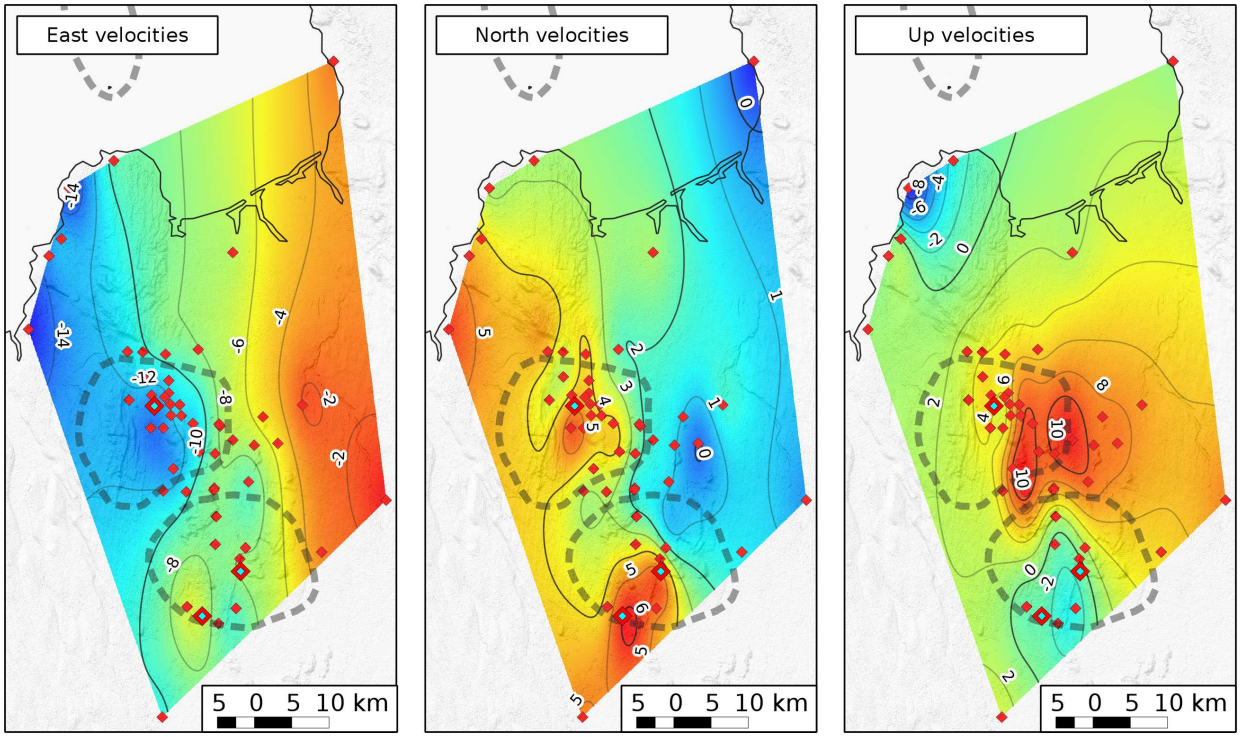

Figure 2.15: GPS velocities interpolation relative to stable Eurasian plate. Velocities are indicated in millimeters per year. Notice that the color scale is not the same between images. Central volcanoes are represented with hatched lines.

The interpolated velocity field shows well the overall gradients in velocities with respect to the East axis. Horizontal velocities are almost zero on the Eurasian plate, but about 14 mm/yr west and 4 mm/yr north on the North-American plate. This is in broad agreement with the NUVEL-1A prediction although the spreading is a bit too slow for stations on the North-American plate. This may relate to strain accumulation across the Húsavík-Flatey fault. The velocity of 18.6 mm/yr in direction 285 degrees anticipated from the NUVEL-1A model corresponds to 18.0 mm/yr in the east component, and 4.8 mm/yr in the north.

On the East velocities map, small anomalies, about 1-2 mm/yr, are noticeable in the following areas: Þeistareykir, Bjarnarflag, and NE of Krafla.

The North velocities also show an East-West gradient with anomalies in Þeistareykir, Bjarnarflag, and NE of Krafla.

The velocity field shows that Bjarnarflag is moving north and east relative to nearby areas and the area NE of Krafla is moving south and west. These kind of anomalies are generally caused by a subsurface pressure decrease located between the anomalies, related also to subsidence. In our case it means that they relate to ongoing pressure decrease around Leirbotnar in Krafla.

The vertical velocity field has three key aspects: Subsidence in Leirbotnar and Bjarnarflag, an important uplift centered on Gjástykki and a local subsidence at a station near the coast in the northwest.

The subsidence south of Krafla is consistent with observations in the area in previous years [Sturkell et al., 2008; Spaans et al., 2012]. The subsidence in Leirbotnar and Bjarnarflag caused by geothermal exploitation is still ongoing. However the broad deformation west of Þeistareykir seems to have changed in shape, now it is essentially an uplift concentrated on a smaller area.

The effect of glacial isostatic adjustment due to the retreat of ice caps in Iceland needs to be taken into account for the region [Árnadóttir et al., 2009; Auriac et al., 2013]. Model predictions indicate a uplift gradient from N-S: with 5 mm/yr uplift rate south of Krafla caldera to 2 mm/yr uplift rate in the Þeistareykir area. When taken into account it shows that the subsidence along the Krafla fissure swarm due to other processes than isostasy, both in the Krafla caldera and in Bjarnarflag, is about 6-7 mm/yr.

Chapter 3

InSAR

3.1 Technology overview

Until 2008, radar images from the ERS and Envisat satellites were acquired over Nothern Iceland. Now that these programs have ended, we have acquired radar data from the TerraSAR-X satellite of the German Space Agency. The satellite signals are of different wavelength:

- ERS: the signal wavelength is about 5.6 cm.
- TerraSAR-X: the signal wavelength is about 3 cm.

Two sets of data are obtained from a radar signal:

- the amplitude image that measures the strength of the signal reflection
- the phase image that contain the signal phase.

Interferomertic Synthetic Aperture Radar (InSAR) analysis use two or more radar images and to measure the difference in phase. The images obtained, called an interferogram, show with fringes displacements in the line of sight (LOS) of the satellite between the two acquisitions. Each fringe represent a displacement of half the satellite wavelength.

At the beginning of the processing we have the following signal components:

$$\Phi_{interferogram} = \Phi_{image1} - \Phi_{image2}$$
$$\Phi_{interferogram} = \Phi_{deformation} + \Phi_{atmospheric} + \Phi_{topographic} + \Phi_{orbital} + \Phi_{noise}$$

When using InSAR for geophysical purposes, only the deformation component has interest. All other components, except the atmospheric one, can be removed when processing a single interferogram.

This atmospheric signal cannot be removed except by methods using the redundancy in the dataset of images, like time series analysis. Interferograms with this signal may show fringes correlated to topography because of atmosphere stratification, and other patterns due to atmospheric turbulences.

Time between the acquisitions has an effect on the amount of displacements that can be measured but also on the image quality, the "coherence". If too large changes occur on the ground during the time between acquisitions, like change in vegetation or erosion, the interferograms may show entire areas only made of noise.

3.2 Data

Since 2009, 14 TerraSAR-X images, distributed in 4 different tracks, have been acquired over Krafla, Gjástykki, Bjarnarflag and Þeistareykir. Four of them have been acquired in 2012. Interferograms can be formed by combining these images (work in progress).

The current TerraSAR-X dataset does not include enough images to do time series analysis. Individual interferograms can though be inspected to evaluate if atmosphere turbulence is likely to be causing unwanted fringes on our interferograms.

Once interfergrams are checked, they will be geocoded and displacements in the line of sight (LOS) of the satellite will be inferred.

Amplitude images of two radar acquisitions are shown in Figs 3.3 and 3.4, but interferograms are needed to evaluate the deformation over North Iceland (work in progress).

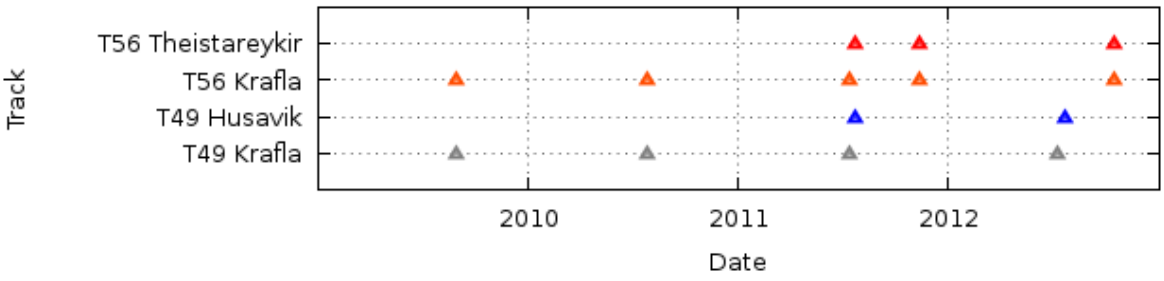

Figure 3.1: TerraSAR-X acquisitions since 2009.

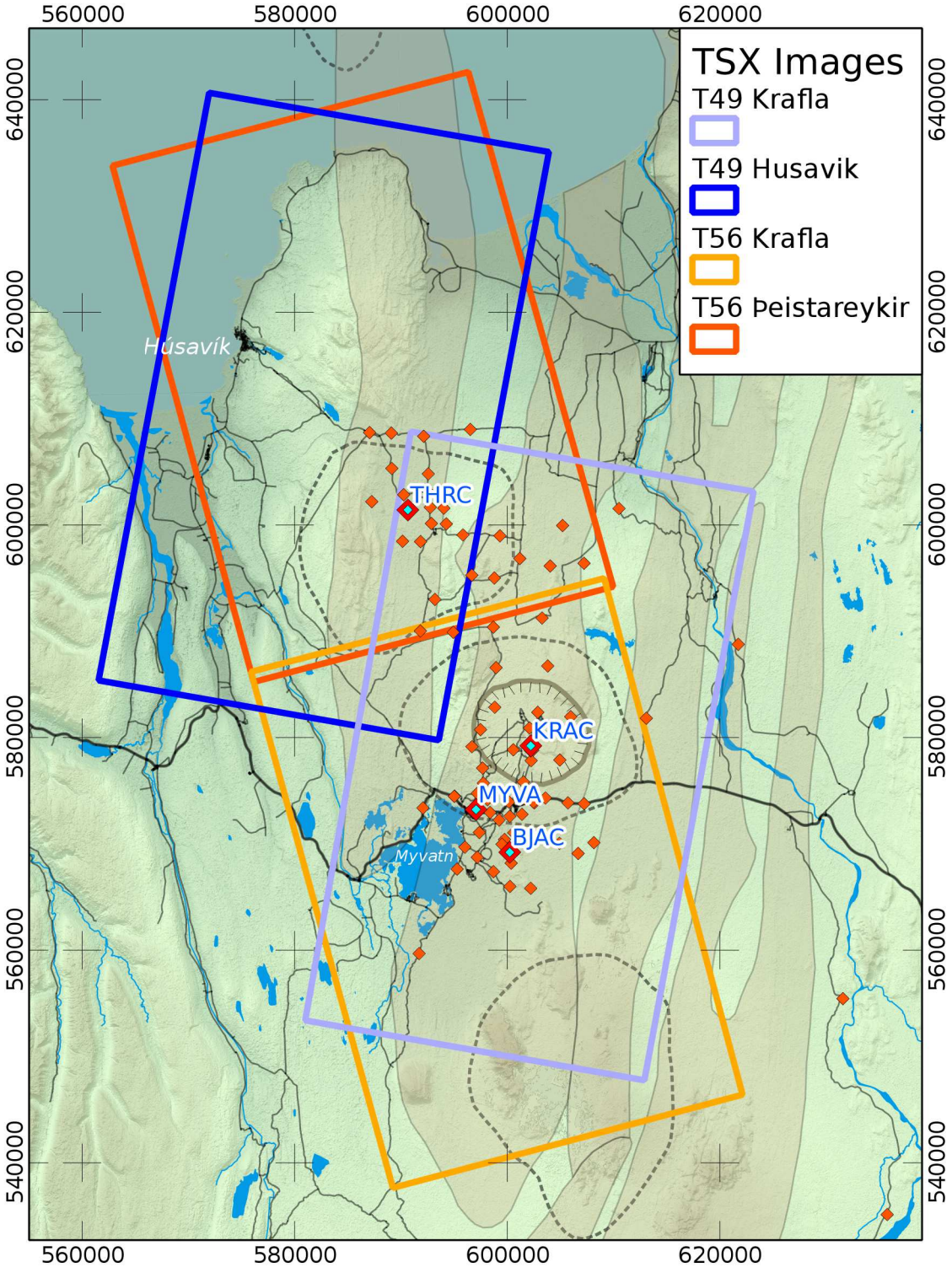

Figure 3.2: Map of the TerraSAR-X images coverage. Map reference system: ISN93. Background is same as Fig 2.1.

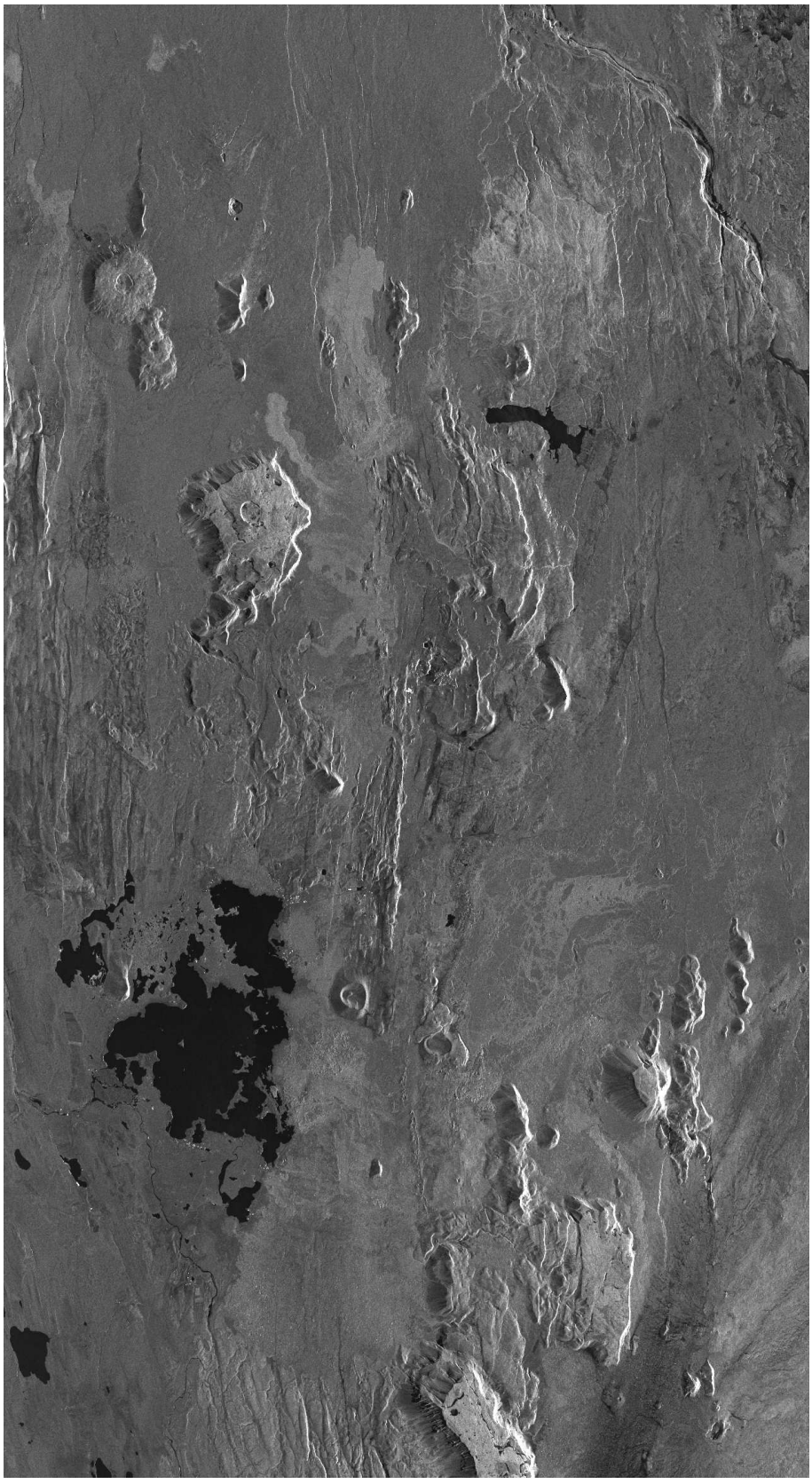

Figure 3.3: TerraSAR-X amplitude image in radar geometry for the track T49 Krafla. See geographical coverage in Figure 3.2

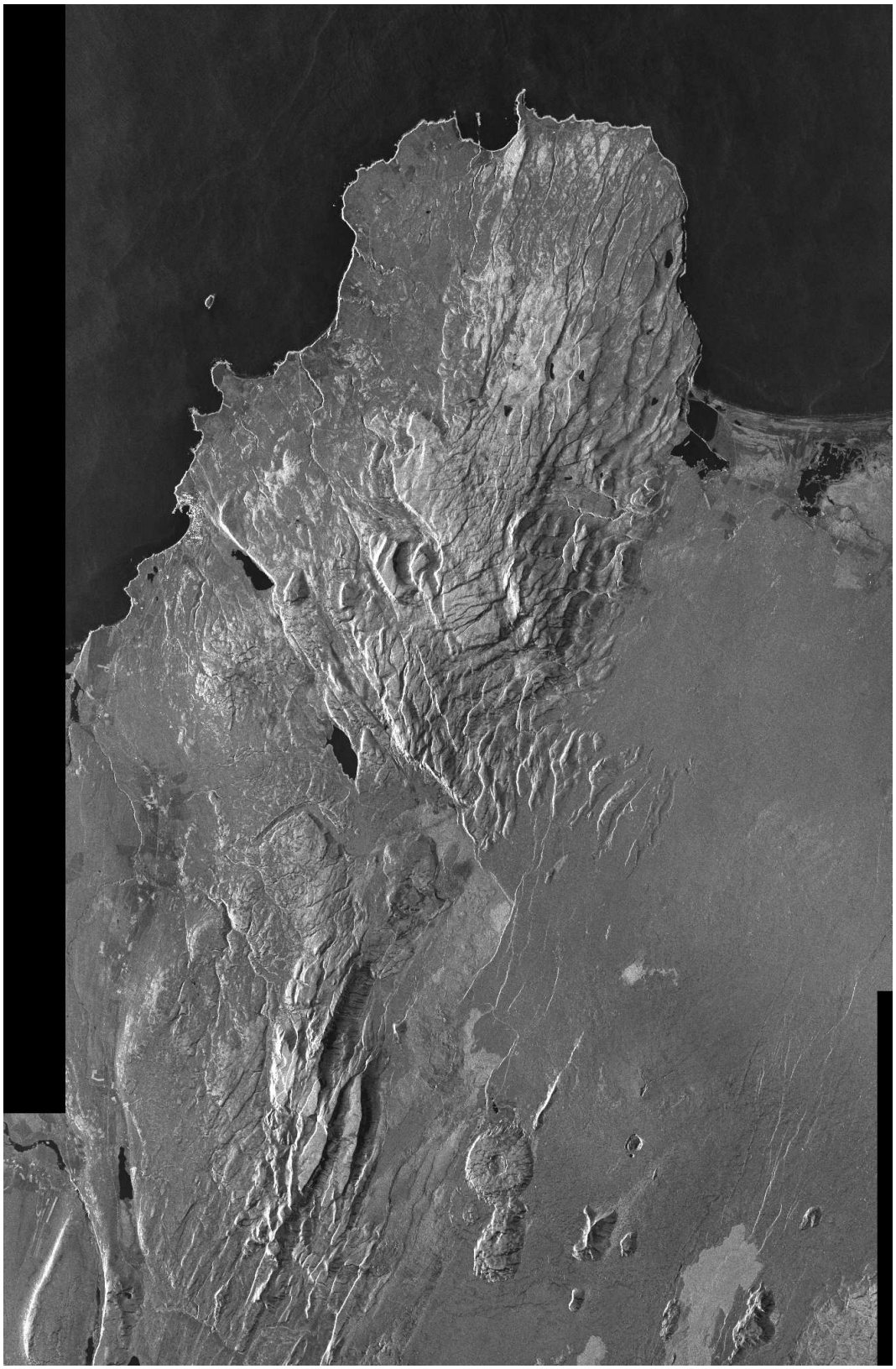

Figure 3.4: TerraSAR-X amplitude image in radar geometry for the track T56 Þeistareykir. See geographical coverage in Figure 3.2

Chapter 4

Acknowledgements

We like to thanks all people who participated in collection of geodetic data, as listed on page 4.

Necessary GPS instruments for this study were provided by Institute of Earth Sciences (IES), UNAVCO and King Abdullah University of Science and Technology (KAUST).

Figures were produced using GRASS, Quantum GIS, and GMT public domain software. GPS data was process using GAMIT/GLOBK software.

References

[Altamimi et al., 2012] Altamimi, Z., Métivier, L., and Collilieux, X. (2012). ITRF2008 plate motion model. *Journal of Geophysical Research*, 117.

[Auriac et al., 2013] Auriac, A., Spaans, K. H., Sigmundsson, F., Hooper, A., Schmidt, P., and Lund, B. (2013). Iceland rising: Solid Earth response to ice retreat inferred from satellite radar interferometry and visocelastic modeling. *Journal of Geophysical Research*, 118.

[Cebecauer et al., 2002] Cebecauer, T., Hofierka, J., and Suri, M. (2002). Processing digital terrain models by regularized spline with tension: tuning interpolation parameters for different input datasets. In *Open source GIS - GRASS users conference*, Trento, Italy.

[DeMets et al., 1990] DeMets, C., Gordon, R. G., Argus, D. F., and Stein, S. (1990). Current plate motions. *Geophysical Journal International*, 101:425–478.

[DeMets et al., 1994] DeMets, C., Gordon, R. G., Argus, D. F., and Stein, S. (1994). Effect of recent revisions to the geomagnetic reversal time scale on estimates of current plate motions. *Geophysical Research Letter*, 21:2191–2194.

[Einarsson and Sæmundsson, 1987] Einarsson, P. and Sæmundsson, K. (1987). Earthquake epicenters 1982-1985 and volcanic systems in Iceland. *Í hlutarins eðli.* edited by Þ. I. Sigfússon, Menningarsjóður, Reykjavík, map accompanying Festschrift for Þorbjörn Sigurgeirsson.

[Herring et al., 2010a] Herring, T. A., King, R. W., and McClusky, S. C. (2010a). *GAMIT Reference Manual : GPS Analysis at MIT.*

[Herring et al., 2010b] Herring, T. A., King, R. W., and McClusky, S. C. (2010b). *GLOBK Reference Manual : Global Kalman filter VLBI and GPS analysis program.*

[Hjartardóttir et al., 2012] Hjartardóttir, A. R., Einarsson, P., Bramham, E., and Wright, T. J. (2012). The Krafla fissure swarm, Iceland, and its formation by rifting events. *Bulletin of Volcanology*, 74:2139–2153.

[Metzger et al., 2011] Metzger, S., Jónsson, S., and Geirsson, S. (2011). Locking depth and slip-rate of the Húsavík Flatey fault, North Iceland, derived from continuous GPS data 2006-2010. *Geophysical Journal International*, 187:564.

[Spaans et al., 2012] Spaans, K., Sigmundsson, F., and Hreinsdóttir, S. (2012). Crustal deformation in the Krafla, Gjástykki and Þeistareykir areas inferred using GPS and InSAR techniques, Status report for 2011. *Landsvirkjun report LV-2012-028, Nordic Volcanological Center, Institute of Earth Sciences Report 1201, University of Iceland.*

[Sturkell et al., 2008] Sturkell, E., Sigmudsson, F., Geirsson, H., Ólafsson, H., and Theodórsson, T. (2008). Multiple volcano deformation sources in a post-rifting period: 1989–2005 behaviour of Krafla, Iceland constrained by levelling, tilt and GPS observations. *Journal of Volcanology and Geothermal Research*, 177:405–417.

[Árnadóttir et al., 2009] Árnadóttir, T., Lund, B., Jiang, W., Geirsson, H., Björnsson, H., and Einarsson, P. (2009). Glacial rebound and plate spreading: results from the first countrywide GPS observations in Iceland. *Geophysical Journal International*, 177:691–716.